Robotica (2018) volume 36, pp. 822–838.
doi:10.1017/S0263574718000061

Robust adaptive output feedback tracking control for flexible-joint robot manipulators based on singularly perturbed decoupling

Huashan Liu* and Yong Huang

College of Information Science and Technology, Donghua University, Shanghai 201620, P.R. China

(Accepted January 8, 2018. First published online: January 31, 2018)

SUMMARY
This paper presents a robust adaptive output feedback tracking controller for the flexible-joint robot manipulators to deal with the unknown upper bounds of parameter uncertainties and external disturbances. With applying the singular perturbation theory and integral manifold concept, the complex nonlinear coupled system of the flexible-joint robot manipulators is divided into a slow subsystem and a fast subsystem. A robust adaptive control scheme based on an improved linear parameterization expression is designed for the slow subsystem, and a saturation function is applied in the robust control term to make the torque output smooth. In the meantime, different from the previous approaches, the second-order derivative term of elastic torque is avoided by using the proposed computed torque method, which simplifies the implementation of the fast control law. Moreover, to carry out the whole control system with only position measurements, an approximate differential filter is involved to generate pseudo velocity signals for links and joint motors. In addition, an explicit but strict stability proof of the control system based on the theory of singularly perturbed systems is presented. Finally, simulation results verify the superior dynamic performance of the proposed controller.

KEYWORDS: Flexible-joint robot, Robust adaptive control, Output feedback control, Singular perturbation, Approximate differentiation.

1. Introduction
Joint flexibility in robot manipulators with joints driven by harmonic reducers or cables (hereafter called flexible-joint robot manipulators) is unavoidable in the dynamics modeling, and severely affects the control performance. Tracking control for such flexible-joint robot manipulators has been receiving increasing attention in the past decades.[1–4]

With respect to adaptive techniques in the area of robot control, taking parametric uncertainties into consideration, Slotine and Li proposed one of the first adaptive tracking controllers for rigid robot manipulators,[5] where the control law consists of a proportional-derivative (PD) control part and a full dynamics feed-forward compensation part, with unknown parameters of the manipulator and its payload being estimated online. However, the presence of flexibility at the joint of most robots, which is characterized by damped oscillations, may lead to poor performance or instability when rigid control strategies are applied directly to the flexible-joint robot manipulators.[5] Taking joint flexibility into account, Spong proposed a rigid-link flexible-joint robot model, which is globally feedback linearizable and reduces to the standard rigid robot model as the joint stiffness tends to infinity.[6,7] As a benchmark, this model has been widely used since then.[8–10] An adaptive controller for flexible-joint robots was developed based on singular perturbation theory and using only position and velocity feedback.[8] Ulrich developed a composite control scheme that consists of a direct model reference adaptive system designed to stabilize the rigid dynamics and a linear correction term to

* Corresponding author. E-mails: hs.liu@qq.com, 1066994564@qq.com

improve damping of vibrations at the joints, in the presence of parametric uncertainties and modeling errors.[9]

Robust adaptive control strategy combines the advantages of the adaptive control and the robust control, and is commonly used to solve the robot control problems considering parametric uncertainties and external disturbances.[11] Fateh proposed a novel robust decentralized controller by the adaptive fuzzy estimation and the compensation of uncertainty for electrically driven robot manipulators, which was proved to be superior in the face of smooth uncertainties.[12] Kolhe *et al.* designed a robust tracking controller based on the uncertainty and disturbance estimation,[13] in which the system nonlinearities, external disturbances, and parametric uncertainties are considered, and a robust observer was proposed to achieve the joint velocity measurements.

It is well known that velocity signals measurements are liable to be contaminated with external noise, moreover, in tracking control situations for robot manipulators, the motor or link velocity sensors are always absent due to hardware cost reduction. Output feedback control, as a technique to make the whole closed-loop system with only measurements of outputs, has aroused some interests in tracking control for flexible-joint robot manipulators.[14–18] Loría and Avila-Becerril developed an output feedback tracking (OFT) controller using back-stepping strategy,[14] in which approximate differentiation was applied to eliminate the link velocity, acceleration and jerk measurements. As presented, the position output feedback was only achieved for the links but not available for the joint motors. In order to estimate the velocities of both links and motors for flexible-joint electronically driven robot manipulators, Yoo *et al.* presented an adaptive observer based OFT controller using the self-recurrent wavelet neural networks (SRWNNs),[15] where the SRWNNs are used to approximate the model uncertainties in dynamics of both slow and fast subsystems. Yoo *et al.* also designed an OFT controller for flexible-joint robot manipulators via the observer dynamic surface design technique, importantly, all the signals in the closed-loop system are guaranteed to be uniformly ultimately bounded.[16] Wang proposed a trajectory tracking controller with only feedback of link angle variables for flexible-joint robot manipulators, where the joint flexibility was regarded as a disturbance to the rigid joint robot manipulators.[18] However, the aforementioned works lay little emphasis on the flexible part of the robot dynamics during the design of the composite controller.[14–16] The OFT methods from the aspect of the rigid part are always considered to achieve the tracking aim, but paying little attention on the dynamic performance of the flexible part of the robot. Actually, for flexible-joint robot manipulators with unknown upper bounds of parametric uncertainties and external disturbances, the flexible part of the robot plays a vital role to influence the oscillation of the joint torque input, and affects the final tracking performance of the robot manipulators.

The main contribution of this work is that a robust adaptive OFT controller is developed by singularly perturbed decoupling, for flexible-joint robot manipulators with unknown upper bounds of parameter uncertainties and external disturbances. First, a robust adaptive control law based on an improved linear parameterization expression, instead of the frequently used parameter linearity method,[5] is proposed for the slow subsystem, to make the parametric estimation more accurate, in terms of linearity model with smaller distortion. Importantly, different from the commonly used sign function,[22] a continuous saturation function is used in the robust control term to make the torque output smooth. On the other side, by deforming the commonly used expression of the fast subsystem,[6,7,17] the control objective becomes a typical tracking issue, which makes the controller design for fast subsystem more flexible. As a second contribution, an approximate differential filter is applied in both slow and fast subsystems to eliminate the velocity measurements completely for both the links and joint motors, so as to achieve an OFT control approach with only position measurements. In addition, the stability analysis for the whole OFT control system is discussed.

The layout of this paper is organized as follows: The dynamics of the flexible-joint manipulators and some useful properties are given in Section 2. In Section 3, by using the singular perturbation theory and integral manifold concept, the full-order nonlinear system is decoupled into a slow subsystem and a fast subsystem. A robust adaptive composite controller with an approximate differential filter is presented in Section 4. Section 5 gives a stability proof of the proposed controller from the perspective of singularly perturbed systems. In Section 6, the simulation comparisons are carried out to evaluate the dynamic performance of the proposed scheme. Finally, some conclusions are given in Section 7.

2. Dynamics of Flexible-Joint Robot Manipulators

The dynamics of n degree-of-freedom flexible-joint robot manipulators are given as[7]

$$\boldsymbol{M}(\boldsymbol{q})\ddot{\boldsymbol{q}} + \boldsymbol{C}(\boldsymbol{q}, \dot{\boldsymbol{q}})\dot{\boldsymbol{q}} + \boldsymbol{G}(\boldsymbol{q}) = \boldsymbol{K}(\boldsymbol{\theta} - \boldsymbol{q}) \tag{1}$$

$$\boldsymbol{J}\ddot{\boldsymbol{\theta}} + \boldsymbol{K}(\boldsymbol{\theta} - \boldsymbol{q}) = \boldsymbol{u} \tag{2}$$

$$\boldsymbol{Z} = \boldsymbol{K}(\boldsymbol{\theta} - \boldsymbol{q}) \tag{3}$$

where $\boldsymbol{q} \in \mathrm{R}^n$ and $\boldsymbol{\theta} \in \mathrm{R}^n$ denote the angular displacements of the link and the motor shafts, respectively, $\boldsymbol{M}(\boldsymbol{q}) \in \mathrm{R}^{n\times n}$ is the symmetric positive definite inertia matrix, $\boldsymbol{C}(\boldsymbol{q}, \dot{\boldsymbol{q}}) \in \mathrm{R}^{n\times n}$ is the centripetal-Coriolis matrix, $\boldsymbol{G}(\boldsymbol{q}) \in \mathrm{R}^n$ is the gravity vector, $\boldsymbol{K} \in \mathrm{R}^{n\times n}$ is a diagonal positive definite matrix representing the joint stiffness, $\boldsymbol{J} \in \mathrm{R}^{n\times n}$ is the inertia matrix of the motors, and $\boldsymbol{u} \in \mathrm{R}^n$ is the control input vector of motor torque, and $\boldsymbol{Z} \in \mathrm{R}^n$ is the elastic torque vector at joint.

Assuming that all the stiffness coefficients k_i are of the same order of magnitude, and they are written as multiples of a single large parameter k, namely,[7]

$$\boldsymbol{K} = k\tilde{\boldsymbol{K}} \tag{4}$$

where $\boldsymbol{K} = \mathrm{diag}\{k_1, \ldots, k_n\}$, $\tilde{\boldsymbol{K}} = \mathrm{diag}\{\tilde{k}_1, \ldots, \tilde{k}_n\}$. Without loss of generality, $\tilde{\boldsymbol{K}} = \mathbf{I}$ is set to simplify the expressions.

The following three properties will be used in the controller design and the stability analysis of system.[5]

Property 1: $\boldsymbol{M}(\boldsymbol{q})$ is a symmetric and positive definite matrix.

Property 2: For an arbitrary vector $\boldsymbol{x} \in \mathrm{R}^n$, there exists

$$\boldsymbol{x}^{\mathrm{T}}[\dot{\boldsymbol{M}}(\boldsymbol{q}) - 2\boldsymbol{C}(\boldsymbol{q}, \dot{\boldsymbol{q}})]\boldsymbol{x} = \mathbf{0} \tag{5}$$

Property 3: Equation (1) can be expressed in a linear parameterization form

$$\boldsymbol{M}(\boldsymbol{q})\ddot{\boldsymbol{q}} + \boldsymbol{C}(\boldsymbol{q}, \dot{\boldsymbol{q}})\dot{\boldsymbol{q}} + \boldsymbol{G}(\boldsymbol{q}) = \boldsymbol{Y}(\boldsymbol{q}, \dot{\boldsymbol{q}}, \ddot{\boldsymbol{q}})\boldsymbol{P} \tag{6}$$

where $\boldsymbol{P} \in \mathrm{R}^r$ is the vector of robot parameters, and $\boldsymbol{Y}(\boldsymbol{q}, \dot{\boldsymbol{q}}, \ddot{\boldsymbol{q}})$ is the corresponding matrix of the known functions.

To facilitate the expressions, $\boldsymbol{M}, \boldsymbol{C}$ and $\boldsymbol{G}$ are used to replace $\boldsymbol{M}(\boldsymbol{q}), \boldsymbol{C}(\boldsymbol{q}, \dot{\boldsymbol{q}})$ and, $\boldsymbol{G}(\boldsymbol{q})$, respectively.

3. The Singular Perturbation System Model

In this section, the full-order nonlinear system described by (1), (2) and (3) is decoupled into a slow subsystem and a fast subsystem in the form of singularly perturbed systems, which makes the controller design for the complex full-order system change into relative simple sub-controllers design of two subsystems.

With multiplying both sides of (1) by $\boldsymbol{M}^{-1}$ and substituting (3) into it, we get

$$\ddot{\boldsymbol{q}} = \boldsymbol{a}_1\dot{\boldsymbol{q}} + \boldsymbol{a}_2\boldsymbol{G} + \boldsymbol{A}_1\boldsymbol{Z} \tag{7}$$

where $\boldsymbol{a}_1 = -\boldsymbol{M}^{-1}\boldsymbol{C}, \boldsymbol{a}_2 = -\boldsymbol{M}^{-1}, \boldsymbol{A}_1 = \boldsymbol{M}^{-1}$.

Defining the perturbation parameter μ=$1/k$, and substituting (2) and (7) into (3), we obtain

$$\mu\ddot{\boldsymbol{Z}} = -\boldsymbol{a}_1\dot{\boldsymbol{q}} - \boldsymbol{a}_2\boldsymbol{G} + \boldsymbol{B}_2\boldsymbol{u} + \boldsymbol{A}_2\boldsymbol{Z} \tag{8}$$

where $\boldsymbol{A}_2 = -(\boldsymbol{J}^{-1} + \boldsymbol{M}^{-1}), \boldsymbol{B}_2 = \boldsymbol{J}^{-1}$.

Remark 1. Equations (7) and (8) compose the singularly perturbed model of the standard form, which is a coupled nonlinear system, it is not likely to prove tractable for analysis or for control-system

https://doi.org/10.1017/S0263574718000061 Published online by Cambridge University Press

design without simplification.[7] By utilizing the concept of integral manifold, a more usable expression derived from (7) and (8), which has the same dimension as the rigid system and incorporates the effects of the joint flexibility, will be obtained in the following part.

3.1. Slow subsystem

Note that, when $\mu \to 0$, i.e., $k \to \infty$, it results in $\boldsymbol{\theta} \to \boldsymbol{q}$, and the control torque $\boldsymbol{u}$ becomes the slow control law $\boldsymbol{u}_s$. We get the slow subsystem from (1), (2) and (3).

$$(\boldsymbol{M} + \boldsymbol{J})\ddot{\boldsymbol{q}} + \boldsymbol{C}\dot{\boldsymbol{q}} + \boldsymbol{G} = \boldsymbol{u}_s \tag{9}$$

Equation (9) indicates the rigid part of the flexible-joint robot manipulators, and is essentially equivalent to the model of rigid robots. Thus, the controller design for the slow subsystem can refer to the methods for the rigid robots.

3.2. Fast subsystem

Since the flexible effect at the joint is non-negligible, the presence of flexibility at joints may produce increasing oscillations, and even leads to system instability. Next, the fast subsystem will be introduced.

Firstly, the form of integral manifold for the system (7) and (8) is defined as

$$\boldsymbol{Z} = \boldsymbol{h}(\boldsymbol{q}, \dot{\boldsymbol{q}}, \boldsymbol{u}, \mu) \tag{10}$$

For convenience, $\boldsymbol{h}$ is used to replace $\boldsymbol{h}(\boldsymbol{q}, \dot{\boldsymbol{q}}, \boldsymbol{u}, \mu)$.

Expanding $\boldsymbol{u}$ and $\boldsymbol{Z}$ in power series, respectively[13,14]

$$\boldsymbol{Z} = \boldsymbol{h}_0 + \mu\boldsymbol{h}_1 + \mu^2\boldsymbol{h}_2 + \cdots + \mu^n\boldsymbol{h}_n + \cdots \tag{11}$$

$$\boldsymbol{u} = \boldsymbol{u}_0 + \mu\boldsymbol{u}_1 + \mu^2\boldsymbol{u}_2 + \cdots + \mu^n\boldsymbol{u}_n + \cdots \tag{12}$$

where $\boldsymbol{h}_0$ represents the desired elastic torque, and $\boldsymbol{u}_0$ indicates the slow control law, namely $\boldsymbol{u}_s$.

Setting $\mu = 0$ in (11) and (12), and substituting them and (10) into (8), we get

$$\mu\ddot{\boldsymbol{h}}_0 = -\boldsymbol{a}_1\dot{\boldsymbol{q}} - \boldsymbol{a}_2\boldsymbol{G} + \boldsymbol{B}_2\boldsymbol{u}_0 + \boldsymbol{A}_2\boldsymbol{h}_0 \tag{13}$$

Defining the elastic torque error as

$$\boldsymbol{\eta} = \boldsymbol{h}_0 - \boldsymbol{Z} \tag{14}$$

From (13) and (8), the fast subsystem is obtained as

$$\mu\ddot{\boldsymbol{\eta}} = -(\boldsymbol{J}^{-1} + \boldsymbol{M}^{-1})\boldsymbol{\eta} - \boldsymbol{J}^{-1}\boldsymbol{u}_f \tag{15}$$

where the fast control law $\boldsymbol{u}_f$ can be expanded as

$$\boldsymbol{u}_f = \mu\boldsymbol{u}_1 + \mu^2\boldsymbol{u}_2 + \cdots + \mu^n\boldsymbol{u}_n + \cdots \tag{16}$$

It is a typical method for almost all of the previous literatures[6,7,17] to focus on (15) to design the fast control law. Differently, in this paper, we will change the form of the fast system (15) by substituting (14) into it:

$$\mu\ddot{\boldsymbol{Z}} = -(\boldsymbol{J}^{-1} + \boldsymbol{M}^{-1})\boldsymbol{Z} - \boldsymbol{J}^{-1}\boldsymbol{u}_f^* \tag{17}$$

where $\boldsymbol{u}_f^*$ represents the new fast control law based on the reshaped fast system (17) from (15), and the relationship between $\boldsymbol{u}_f$ and $\boldsymbol{u}_f^*$ is given as

$$\boldsymbol{u}_f^* = -\boldsymbol{u}_f - \mu\boldsymbol{J}\ddot{\boldsymbol{h}}_0 - \boldsymbol{J}(\boldsymbol{J}^{-1} + \boldsymbol{M}^{-1})\boldsymbol{h}_0 \tag{18}$$

https://doi.org/10.1017/S0263574718000061 Published online by Cambridge University Press

Remarkably, without considering the error term $\boldsymbol{\eta}$, (17) is actually a fast subsystem to enable $\boldsymbol{Z}$ to track $\boldsymbol{h}_0$, which makes the design of the control law more feasible than (15).

Remark 2. As presented in refs. [14–16], the velocity signal of the motor is not necessary in the output feedback control, but the corresponding controllers for the flexible part are all designed with only the torque-feedback based proportional terms, which always fails to restrain the oscillation efficiently at the joints.

By deforming the frequently used fast system (15) in the previous literatures,[6,7,17] the design of the fast control law becomes into a typical tracking issue described by (17) and (18). Hence, mature tracking methods (classic PID control, computed torque control, sliding mode control, neural networked control, etc.) adopted in the area of rigid robot manipulators can be used for the purpose of solving such issue, facilitating the design of the fast control law.

4. Design of Robust Adaptive Controller

By using a combination of singular perturbation theory and integral manifold concept, we get the slow and fast subsystems as presented above. Specifically, the slow subsystem is used to represent the dynamics of the rigid part of the flexible-joint robot manipulators (its expression is same to that of rigid robot manipulators), and the fast subsystem indicates the flexible dynamics caused by the joints. After deformation of the original fast subsystem (15), the system control can be regarded as to solve two typical tracking issues, where the slow subsystem settles the tracking of link angle (almost the same with the tracking problem exists in the pure rigid robot manipulators), and the fast subsystem handles the tracking of the elastic torque at the joints. This decoupling treatment on the original complex dynamics of the flexible-joint robot manipulator facilitates the controller design, i.e., the sub-controllers for each subsystem can be designed and implemented separately.

4.1. Control goal

The controller design is based on the reshaped singularly perturbed system (9) and (17). Assuming the stiffness at the joint is large enough, to handle the issue of uncertainty of model error with unknown bound and external disturbances, a robust adaptive controller to guarantee the joint angular displacements converge to the desired is designed. Given desired trajectory in joint space $\boldsymbol{q}_\mathrm{d} \in \mathrm{R}^n$, $\boldsymbol{q}_\mathrm{d}$ is assumed to be twice differentiable, $\boldsymbol{q}_\mathrm{d}$ and its first two derivatives are bounded for all $t > 0$. Defining the position tracking error as $\boldsymbol{e} = \boldsymbol{q}_\mathrm{d} - \boldsymbol{q}$, in brief, the control goal can be expressed as follows: $\forall \boldsymbol{e}(0) \in \mathrm{R}^n$, $\lim\limits_{t\to\infty} \boldsymbol{e} = \boldsymbol{0}$.

4.2. Approximate differential filter

Velocity measurements of both links and joint motors for flexible-joint robot manipulators are essential in most of the existing control schemes, i.e., full-state feedback controllers, and noises are often inevitably included in the measurements, degrading the accuracy of the feedback signals and even making the controller unstable, especially at low-speed running situations. Beyond that, the velocity sensors increase the cost of the hardware of the physical system. In this section, an approximate differential filter is applied to generate pseudo velocity feedback from the position signals of links and motors, and guarantees the closed-loop control with only position measurements.

The filter is given as[19]

$$\dot{\boldsymbol{v}} = -\boldsymbol{A}\boldsymbol{y} + \boldsymbol{B}\dot{\bar{\boldsymbol{q}}} \tag{19}$$

which is made up of two implementable parts:

$$\dot{\boldsymbol{y}} = -\boldsymbol{A}\boldsymbol{y} - \boldsymbol{A}\boldsymbol{B}\bar{\boldsymbol{q}} \tag{20}$$

$$\boldsymbol{v} = \boldsymbol{y} + \boldsymbol{B}\bar{\boldsymbol{q}} \tag{21}$$

where $\boldsymbol{v} \in \mathrm{R}^n$ is the approximate velocity signal, $\bar{\boldsymbol{q}}$ is the position signal, $\boldsymbol{y}$ is an auxiliary variable introduced to permit the implementation of the filter without utilizing velocity measurements. $\boldsymbol{A} = \mathrm{diag}\{a_1, a_2, \ldots, a_n\} \in \mathrm{R}^{n\times n}$, $\boldsymbol{B} = \mathrm{diag}\{b_1, b_2, \ldots, b_n\} \in \mathrm{R}^{n\times n}$ are positive definite diagonal constant matrices, a_i and b_i $(i = 1, 2, \ldots, n)$ are positive constants.

Remark 3. With comparisons to the literature,[14–16] the major difference is that the proposed approximate differential filter is used to estimate the velocity signal of the links in the slow subsystem and the velocity signal of the motors in the fast subsystem, respectively, to eliminate the velocity measurements completely and generate pseudo velocity signals as approximations to the actual for both links and motors. This turns the proposed full-state feedback tracking controller into an OFT controller with only position measurements for both links and joint motors. More importantly, the proposed filter helps restrain the initial torque output of the joint motors, especially when there is a non-zero initial position tracking error of the joint, enabling the robot to run more stably. This will be proved in Section 6. In addition, the proposed filter with all positive filtering gains in matrices $\boldsymbol{A}$ and $\boldsymbol{B}$ also makes it easier to guarantee the global asymptotically stability of the system without imposing any restrictions on its bandwidth.

4.3. Slow control law

The slow subsystem can be regarded as the rigid part of the full-order rigid-flexible coupled system. Since the design of the slow sub-controller is based on the slow subsystem, the control strategies for rigid robot manipulators can be used to design the slow sub-controller.

The uncertain model errors and external disturbances are defined as $\boldsymbol{w} \in \mathrm{R}^n$, and then (1) in the dynamic model of the flexible-joint robots can be rewritten as

$$\boldsymbol{M}\ddot{\boldsymbol{q}} + \boldsymbol{C}\dot{\boldsymbol{q}} + \boldsymbol{G} + \boldsymbol{w} = \boldsymbol{K}(\boldsymbol{\theta} - \boldsymbol{q}) \tag{22}$$

The norm of $\boldsymbol{w}$ satisfies $\|\boldsymbol{w}\| \leq d_1 + d_2\|\boldsymbol{e}\| + d_3\|\dot{\boldsymbol{e}}\|$, where d_1, d_2, d_3 are all positive constants.[20] We get

$$\|\boldsymbol{w}\| \leq \boldsymbol{d}^{\mathrm{T}}\boldsymbol{f} \tag{23}$$

where $\boldsymbol{d} = (\,d_1\ d_2\ d_3\,)^{\mathrm{T}}$, $\boldsymbol{f} = (\,1\ \|\boldsymbol{e}\|\ \|\dot{\boldsymbol{e}}\|\,)^{\mathrm{T}}$.

The corresponding standard singularly perturbed model can also be rewritten as

$$\ddot{\boldsymbol{q}} = \boldsymbol{a}_1\dot{\boldsymbol{q}} + \boldsymbol{a}_2\boldsymbol{G} + \boldsymbol{a}_2\boldsymbol{w} + \boldsymbol{A}_1\boldsymbol{Z} \tag{24}$$

$$\mu\ddot{\boldsymbol{Z}} = -\boldsymbol{a}_1\dot{\boldsymbol{q}} - \boldsymbol{a}_2\boldsymbol{G} - \boldsymbol{a}_2\boldsymbol{w} + \boldsymbol{B}_2\boldsymbol{u} + \boldsymbol{A}_2\boldsymbol{Z} \tag{25}$$

Combining (2), (3) and (22), the new slow subsystem is presented as

$$(\boldsymbol{M} + \boldsymbol{J})\ddot{\boldsymbol{q}} + \boldsymbol{C}\dot{\boldsymbol{q}} + \boldsymbol{G} + \boldsymbol{w} = \boldsymbol{u}_{\mathrm{s}} \tag{26}$$

Define the virtual desired trajectory

$$\boldsymbol{q}_{\mathrm{r}} = \boldsymbol{q}_{\mathrm{d}} + \boldsymbol{\Lambda}\int_0^t \boldsymbol{e}dt \tag{27}$$

where $\boldsymbol{\Lambda} \in \mathrm{R}^{n\times n}$ is a constant matrix with its eigenvalues strictly located in the right half of the complex plane.

Accordingly, we have

$$\dot{\boldsymbol{q}}_{\mathrm{r}} = \dot{\boldsymbol{q}}_{\mathrm{d}} + \boldsymbol{\Lambda}\boldsymbol{e} \tag{28}$$

$$\ddot{\boldsymbol{q}}_{\mathrm{r}} = \ddot{\boldsymbol{q}}_{\mathrm{d}} + \boldsymbol{\Lambda}\dot{\boldsymbol{e}} \tag{29}$$

$$\boldsymbol{s} = \dot{\boldsymbol{q}}_{\mathrm{r}} - \dot{\boldsymbol{q}} = \dot{\boldsymbol{e}} + \boldsymbol{\Lambda}\boldsymbol{e} \tag{30}$$

Usually, the slow subsystem cannot be linearized directly, and it is a general method as (6) to utilize the parameter linearity of the rigid robots to replace it approximately.[5] But this method leads to modeling error and deteriorates estimation accuracy of the system parameters.[21] Motivated by ref. [8], we use an improved linear parameterization expression in the adaptive control to make the estimation more accurate to the practical situations:

$$\boldsymbol{M}(\ddot{\boldsymbol{q}}_{\rm r} + \lambda_{\rm c}\boldsymbol{s}) + \boldsymbol{C}\dot{\boldsymbol{q}}_{\rm r} + \boldsymbol{G} = \boldsymbol{Y}(\boldsymbol{q}, \dot{\boldsymbol{q}}, \dot{\boldsymbol{q}}_{\rm r}, \ddot{\boldsymbol{q}}_{\rm r} + \lambda_{\rm c}\boldsymbol{s})\boldsymbol{P} \tag{31}$$

$$\hat{\boldsymbol{M}}(\ddot{\boldsymbol{q}}_{\rm r} + \lambda_{\rm c}\boldsymbol{s}) + \hat{\boldsymbol{C}}\dot{\boldsymbol{q}}_{\rm r} + \hat{\boldsymbol{G}} = \boldsymbol{Y}(\boldsymbol{q}, \dot{\boldsymbol{q}}, \dot{\boldsymbol{q}}_{\rm r}, \ddot{\boldsymbol{q}}_{\rm r} + \lambda_{\rm c}\boldsymbol{s})\hat{\boldsymbol{P}} \tag{32}$$

where $\boldsymbol{Y}(\boldsymbol{q}, \dot{\boldsymbol{q}}, \dot{\boldsymbol{q}}_{\rm r}, \ddot{\boldsymbol{q}}_{\rm r} + \lambda_{\rm c}\boldsymbol{s})$ (written as $\boldsymbol{Y}$ for short), is the corresponding matrix function of knows, $\hat{\boldsymbol{P}}$ is the time-varying estimation of robot parameter $\boldsymbol{P}$, $\hat{\boldsymbol{M}}$, $\hat{\boldsymbol{C}}$ and $\hat{\boldsymbol{G}}$ indicate the estimation of $\boldsymbol{M}, \boldsymbol{C}, \boldsymbol{G}$ and $\lambda_{\rm c}$ is a positive constant.

We propose a robust adaptive controller as

$$\boldsymbol{u}_{\rm s} = (\hat{\boldsymbol{M}} + \hat{\boldsymbol{J}})(\ddot{\boldsymbol{q}}_{\rm r} + \lambda_{\rm c}\boldsymbol{s}) + \hat{\boldsymbol{C}}\dot{\boldsymbol{q}}_{\rm r} + \hat{\boldsymbol{G}} - \boldsymbol{K}\boldsymbol{s} + \boldsymbol{\Phi} \tag{33}$$

where $\boldsymbol{K} = \lambda_{\rm c}(\boldsymbol{M} + \boldsymbol{J}) - \boldsymbol{K}_{\rm s}$, $\boldsymbol{K}_{\rm s}$ is a positive definite matrix, and $\boldsymbol{\Phi}$ is the robust control term defined as

$$\boldsymbol{\Phi} = \begin{cases} \dfrac{1}{m_1}\hat{\boldsymbol{d}}^{\rm T}\boldsymbol{f}\cdot \mathrm{sat}(\boldsymbol{s}), & \forall \|\boldsymbol{s}\| > l_1 \\ \dfrac{1}{M_1}\hat{\boldsymbol{d}}^{\rm T}\boldsymbol{f}\cdot \mathrm{sat}(\boldsymbol{s}), & \forall \|\boldsymbol{s}\| \le l_1 \end{cases} \tag{34}$$

where sat$(\cdot)$ represents a class of saturation functions, and m_1, l_1 are positive constants with $m_1 = M_1 l_1$.

Here, the saturation function proposed in ref. [22] is applied.

$$\mathrm{sat}(\cdot) = \begin{cases} m_1 \cdot \mathrm{sign}(\cdot), & \forall \|\cdot\| > l_1 \\ M_1 \cdot (\cdot) \quad , & \forall \|\cdot\| \le l_1 \end{cases} \tag{35}$$

where $\mathrm{sign}(\cdot) = \begin{cases} 1, & \cdot > 0 \\ 0, & \cdot = 0 \\ -1, & \cdot < 0 \end{cases}$.

Define $(\tilde{\cdot}) = (\cdot) - (\hat{\cdot})$, $(\cdot)$ is the true value, $(\hat{\cdot})$ indicates the estimated value and $(\tilde{\cdot})$ represents the estimated error of the true value.

The adaptive control laws are given as

$$\dot{\hat{\boldsymbol{P}}} = \boldsymbol{\Gamma}^{-1}(\boldsymbol{Y}\boldsymbol{s} + \boldsymbol{\Gamma}\tilde{\boldsymbol{P}}) \tag{36}$$

$$\dot{\hat{\boldsymbol{d}}} = \begin{cases} \boldsymbol{\Gamma_d}^{-1}(\boldsymbol{f}\,\|\boldsymbol{s}\| - \boldsymbol{a}\hat{\boldsymbol{d}}), & \forall \|\boldsymbol{s}\| > l_1 \\ \boldsymbol{\Gamma_d}^{-1}(\boldsymbol{f}\|\boldsymbol{s}\|^2 - \boldsymbol{a}\hat{\boldsymbol{d}}), & \forall \|\boldsymbol{s}\| \le l_1 \end{cases} \tag{37}$$

where $\boldsymbol{\Gamma} \in \mathrm{R}^{5\times 5}$, $\boldsymbol{\Gamma_d} \in \mathrm{R}^{3\times 3}$ and $\boldsymbol{a} \in \mathrm{R}^{3\times 3}$ are all positive definite diagonal constant matrices. Equations (36) and (37) are used to estimate the coefficients for each error items.

To generate the pseudo velocity error of link in the slow subsystem, the aforementioned approximate differential filter is applied as

$$\dot{\boldsymbol{v}}_1 = -\boldsymbol{A}_1\boldsymbol{v}_1 + \boldsymbol{B}_1\dot{\boldsymbol{e}} \tag{38}$$

where $\boldsymbol{v}_1$ represents the pseudo velocity error of links, and both $\boldsymbol{A}_1$ and $\boldsymbol{B}_1$ are positive definite diagonal constant matrices.

Remark 4. With regard to the unknown uncertainty bound, for the slow subsystem, a robust adaptive slow sub-controller (33) is designed. It consists of a feed-forward control term, a PD control term and a robust control term. The robust control term makes the errors resulted from the model and external disturbances always limited in a certain range by using the saturation function, and enables the control error of the slow subsystem globally uniformly ultimately bounded (this will be proved in the stability analysis part).

4.4. Fast control law

The existing solutions to fast control law often adopt torque-feedback based classic pure proportional or PD control, which is limited to suppress the overshoot. This results in oscillations at the joints and negative effect to the tracking performance, especially when there is a non-zero initial tracking error. Aiming at solving this problem, we redesigned the fast control law with considering the output feedback strategy.

In this paper, the fast control law is proposed as

$$\boldsymbol{u}_{\mathrm{f}}^{*} = -\boldsymbol{J}\mu(\ddot{\boldsymbol{h}}_0 + \boldsymbol{k}_{\mathrm{p}}\boldsymbol{\eta} + \boldsymbol{k}_{\mathrm{v}}\dot{\boldsymbol{\eta}}) - \boldsymbol{J}(\boldsymbol{J}^{-1} + \boldsymbol{M}^{-1})\boldsymbol{Z} \tag{39}$$

where both $\boldsymbol{k}_{\mathrm{p}} \in \mathrm{R}^{n\times n}$ and $\boldsymbol{k}_{\mathrm{v}} \in \mathrm{R}^{n\times n}$ are constant diagonal matrices.

Substitute (39) into (18)

$$\boldsymbol{u}_{\mathrm{f}} = \boldsymbol{K}_{\mathrm{P}}\boldsymbol{\eta} + \boldsymbol{K}_{\mathrm{D}}\dot{\boldsymbol{\eta}} \tag{40}$$

where $\boldsymbol{K}_{\mathrm{P}} = \boldsymbol{J}\mu\boldsymbol{k}_{\mathrm{p}} - \boldsymbol{J}(\boldsymbol{J}^{-1} + \boldsymbol{M}^{-1})$, $\boldsymbol{K}_{\mathrm{D}} = \boldsymbol{J}\mu\boldsymbol{k}_{\mathrm{v}}$.

In respect of the output feedback problem for the fast subsystem, the pseudo differential of the elastic torque error is created by the approximate differential filter that

$$\dot{\boldsymbol{v}}_2 = -\boldsymbol{A}_2\boldsymbol{v}_2 + \boldsymbol{B}_2\dot{\boldsymbol{\eta}} \tag{41}$$

where $\boldsymbol{v}_2$ is the pseudo differential of the elastic torque error, and both $\boldsymbol{A}_2$ and $\boldsymbol{B}_2$ are positive definite diagonal constant matrices.

Remark 5. The exact robot dynamics model based computed torque control approaches can be taken as in a composite form of feed-forward controller and PD controller. $-\boldsymbol{J}(\boldsymbol{J}^{-1} + \boldsymbol{M}^{-1})\boldsymbol{Z} - \boldsymbol{J}\mu\ddot{\boldsymbol{h}}_0$ is the feed-forward term and $-\boldsymbol{J}\mu(\boldsymbol{k}_{\mathrm{p}}\boldsymbol{\eta} + \boldsymbol{k}_{\mathrm{v}}\dot{\boldsymbol{\eta}})$ is the PD term in (39), where the feed-forward part is to track the target elastic torque and the PD part is used to provide the torque to eliminate tracking error. Moreover, compared to the previous controller design for the flexible part in output feedback control,[14–16] the proposed controller (40) is more flexible in the design of the control law and can adopt various control methods including computed torque approach according to different control goals.

Note that, $\boldsymbol{K}_{\mathrm{P}}$ in (40) is a time-varying matrix, and it seems like to make the control scheme more complex, but considering that the changing of $\boldsymbol{J}(\boldsymbol{J}^{-1} + \boldsymbol{M}^{-1})$ is slow and its corresponding value is much smaller in comparison to $\boldsymbol{J}\mu\boldsymbol{k}_{\mathrm{p}}$, then a proper constant matrix can be chosen in practical application such that the asymptotically stability of the fast subsystem is guaranteed.

The block diagram of the proposed controller is shown in Fig. 1.

5. Stability Analysis

In this section, we will analyze the stability of the slow subsystem, the fast subsystem and the whole composite system in sequence with considering the approximate differential filter.[18]

5.1. Stability analysis of the slow system

For slow subsystem, the Lyapunov function candidate V_1 is defined as

$$V_1 = \frac{1}{2}\boldsymbol{s}^{\mathrm{T}}(\boldsymbol{M} + \boldsymbol{J})\boldsymbol{s} + \frac{1}{2}\tilde{\boldsymbol{P}}^{\mathrm{T}}\boldsymbol{\Gamma}\tilde{\boldsymbol{P}} + \frac{1}{2}\boldsymbol{v}_1^{\mathrm{T}}\boldsymbol{v}_1 + \frac{1}{2}\tilde{\boldsymbol{d}}^{\mathrm{T}}\boldsymbol{\Gamma}_d\tilde{\boldsymbol{d}} \tag{42}$$

It can be rewritten in matrix form as $V_1 = \frac{1}{2}\boldsymbol{X}^{\mathrm{T}}\boldsymbol{\Omega}\boldsymbol{X}$, where $\boldsymbol{X} = \begin{pmatrix} \boldsymbol{s} \\ \boldsymbol{v}_1 \\ \tilde{\boldsymbol{P}} \\ \tilde{\boldsymbol{d}} \end{pmatrix}$, $\boldsymbol{\Omega} = \begin{pmatrix} \boldsymbol{M}+\boldsymbol{J} & 0 & 0 & 0 \\ 0 & 1 & 0 & 0 \\ 0 & 0 & \boldsymbol{\Gamma} & 0 \\ 0 & 0 & 0 & \boldsymbol{\Gamma}_d \end{pmatrix}$. Obviously, V_1 is positive definite.

In order to facilitate the proof, V_1 is partitioned as $V_1 = V_0 + \frac{1}{2}\tilde{\boldsymbol{d}}^{\mathrm{T}}\boldsymbol{\Gamma}_d\tilde{\boldsymbol{d}}$, where $V_0 = \frac{1}{2}\boldsymbol{s}^{\mathrm{T}}(\boldsymbol{M} + \boldsymbol{J})\boldsymbol{s} + \frac{1}{2}\tilde{\boldsymbol{P}}^{\mathrm{T}}\boldsymbol{\Gamma}\tilde{\boldsymbol{P}} + \frac{1}{2}\boldsymbol{v}_1^{\mathrm{T}}\boldsymbol{v}_1$.

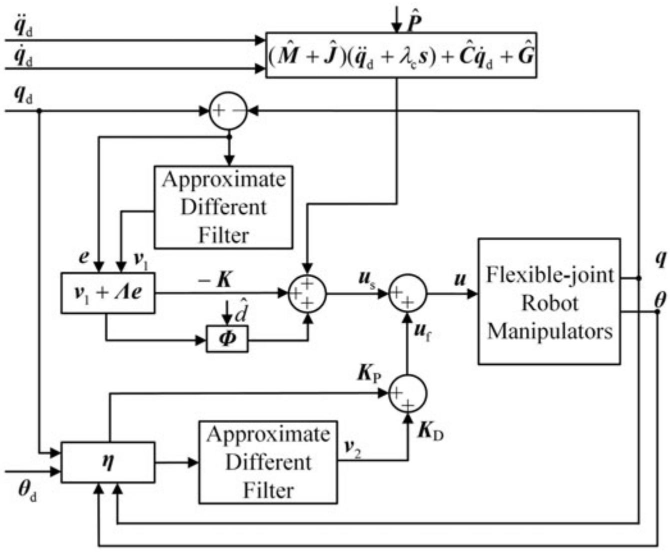

Fig. 1. Block diagram of the proposed controller.

Taking the derivative of V_1 with respect to time, and substitute (26), (33) and (36) into V_0, we get

$$\begin{aligned}
\dot{V}_0 &= \boldsymbol{s}^{\mathrm{T}}(\boldsymbol{M}+\boldsymbol{J})\dot{\boldsymbol{s}}+\frac{1}{2}\boldsymbol{s}^{\mathrm{T}}\dot{\boldsymbol{M}}\boldsymbol{s}+\tilde{\boldsymbol{P}}^{\mathrm{T}}\boldsymbol{\Gamma}\dot{\tilde{\boldsymbol{P}}}+\boldsymbol{v}_1^{\mathrm{T}}\dot{\boldsymbol{v}}_1\\
&= \boldsymbol{s}^{\mathrm{T}}(\boldsymbol{M}+\boldsymbol{J})(\ddot{\boldsymbol{q}}_{\mathrm{r}}-\ddot{\boldsymbol{q}})+\frac{1}{2}\boldsymbol{s}^{\mathrm{T}}\dot{\boldsymbol{M}}\boldsymbol{s}+\tilde{\boldsymbol{P}}^{\mathrm{T}}\boldsymbol{\Gamma}\dot{\tilde{\boldsymbol{P}}}+\boldsymbol{v}_1{}^{\mathrm{T}}\dot{\boldsymbol{v}}_1\\
&= \boldsymbol{s}^{\mathrm{T}}\left[(\boldsymbol{M}+\boldsymbol{J})\ddot{\boldsymbol{q}}_{\mathrm{r}}-(\boldsymbol{u}_{\mathrm{s}}-\boldsymbol{C}\dot{\boldsymbol{q}}-\boldsymbol{G}-\boldsymbol{w})\right]+\frac{1}{2}\boldsymbol{s}^{\mathrm{T}}\dot{\boldsymbol{M}}\boldsymbol{s}+\tilde{\boldsymbol{P}}^{\mathrm{T}}\boldsymbol{\Gamma}\dot{\tilde{\boldsymbol{P}}}+\boldsymbol{v}_1^{\mathrm{T}}\dot{\boldsymbol{v}}_1\\
&= \boldsymbol{s}^{\mathrm{T}}\left[(\boldsymbol{M}+\boldsymbol{J})\ddot{\boldsymbol{q}}_{\mathrm{r}}-(\hat{\boldsymbol{M}}+\hat{\boldsymbol{J}})(\ddot{\boldsymbol{q}}_{\mathrm{r}}+\lambda_{\mathrm{c}}\boldsymbol{s})-\hat{\boldsymbol{C}}\dot{\boldsymbol{q}}_{\mathrm{r}}-\hat{\boldsymbol{G}}+\boldsymbol{K}\boldsymbol{s}-\boldsymbol{\Phi}+\boldsymbol{C}\dot{\boldsymbol{q}}+\boldsymbol{G}+\boldsymbol{w})\right]\\
&\quad+\frac{1}{2}\boldsymbol{s}^{\mathrm{T}}\dot{\boldsymbol{M}}\boldsymbol{s}+\tilde{\boldsymbol{P}}^{\mathrm{T}}\boldsymbol{\Gamma}\dot{\tilde{\boldsymbol{P}}}+\boldsymbol{v}_1{}^{\mathrm{T}}\dot{\boldsymbol{v}}_1\\
&= \boldsymbol{s}^{\mathrm{T}}[(\boldsymbol{M}+\boldsymbol{J})\ddot{\boldsymbol{q}}_{\mathrm{r}}-(\hat{\boldsymbol{M}}+\hat{\boldsymbol{J}})(\ddot{\boldsymbol{q}}_{\mathrm{r}}+\lambda_{\mathrm{c}}\boldsymbol{s})-\hat{\boldsymbol{C}}\dot{\boldsymbol{q}}_{\mathrm{r}}-\hat{\boldsymbol{G}}+\lambda_{\mathrm{c}}(\boldsymbol{M}+\boldsymbol{J})\boldsymbol{s}\\
&\quad-\boldsymbol{K}_s\boldsymbol{s}-\boldsymbol{\Phi}+\boldsymbol{C}(\dot{\boldsymbol{q}}_{\mathrm{r}}-\boldsymbol{s})+\boldsymbol{G}+\boldsymbol{w})]+\frac{1}{2}\boldsymbol{s}^{\mathrm{T}}\dot{\boldsymbol{M}}\boldsymbol{s}+\tilde{\boldsymbol{P}}^{\mathrm{T}}\boldsymbol{\Gamma}\dot{\tilde{\boldsymbol{P}}}+\boldsymbol{v}_1^{\mathrm{T}}\dot{\boldsymbol{v}}_1\\
&= \boldsymbol{s}^{\mathrm{T}}[\boldsymbol{Y}\tilde{\boldsymbol{P}}-\boldsymbol{\Phi}-\boldsymbol{K}_s\boldsymbol{s}+\boldsymbol{w}]+\tilde{\boldsymbol{P}}^{\mathrm{T}}\boldsymbol{\Gamma}\dot{\tilde{\boldsymbol{P}}}+\boldsymbol{v}_1^{\mathrm{T}}\dot{\boldsymbol{v}}_1\\
&= \tilde{\boldsymbol{P}}^{\mathrm{T}}(\boldsymbol{Y}^{\mathrm{T}}\boldsymbol{s}+\boldsymbol{\Gamma}\dot{\tilde{\boldsymbol{P}}})-\boldsymbol{s}^{\mathrm{T}}\boldsymbol{\Phi}-\boldsymbol{s}^{\mathrm{T}}\boldsymbol{K}_s\boldsymbol{s}+\boldsymbol{s}^{\mathrm{T}}\boldsymbol{w}+\boldsymbol{v}_1^{\mathrm{T}}\dot{\boldsymbol{v}}_1\\
&= \tilde{\boldsymbol{P}}^{\mathrm{T}}(\boldsymbol{Y}^{\mathrm{T}}\boldsymbol{s}-\boldsymbol{\Gamma}\dot{\hat{\boldsymbol{P}}})-\boldsymbol{s}^{\mathrm{T}}\boldsymbol{\Phi}-\boldsymbol{s}^{\mathrm{T}}\boldsymbol{K}_s\boldsymbol{s}+\boldsymbol{s}^{\mathrm{T}}\boldsymbol{w}+\boldsymbol{v}_1^{\mathrm{T}}\dot{\boldsymbol{v}}_1\\
&= -\tilde{\boldsymbol{P}}^{\mathrm{T}}\boldsymbol{\Gamma}\tilde{\boldsymbol{P}}-\boldsymbol{s}^{\mathrm{T}}\boldsymbol{\Phi}-\boldsymbol{s}^{\mathrm{T}}\boldsymbol{K}_s\boldsymbol{s}+\boldsymbol{s}^{\mathrm{T}}\boldsymbol{w}+\boldsymbol{v}_1^{\mathrm{T}}\dot{\boldsymbol{v}}_1
\end{aligned}\tag{43}$$

When $\|\boldsymbol{s}\| > l_1$, substituting (23), (34) and (35) and into (43)

$$\begin{aligned}
\dot{V}_0 &= -\tilde{\boldsymbol{P}}^{\mathrm{T}}\boldsymbol{\Gamma}\tilde{\boldsymbol{P}}-\boldsymbol{s}^{\mathrm{T}}\hat{\boldsymbol{d}}^{\mathrm{T}}\boldsymbol{f}\cdot\mathrm{sign}(\boldsymbol{s})-\boldsymbol{s}^{\mathrm{T}}\boldsymbol{K}_s\boldsymbol{s}+\boldsymbol{s}^{\mathrm{T}}\boldsymbol{w}+\boldsymbol{v}_1^{\mathrm{T}}\dot{\boldsymbol{v}}_1\\
&\le -\tilde{\boldsymbol{P}}^{\mathrm{T}}\boldsymbol{\Gamma}\tilde{\boldsymbol{P}}-\|\boldsymbol{s}\|\,\hat{\boldsymbol{d}}^{\mathrm{T}}\boldsymbol{f}-\boldsymbol{s}^{\mathrm{T}}\boldsymbol{K}_s\boldsymbol{s}+\|\boldsymbol{s}\|\,\boldsymbol{d}^{\mathrm{T}}\boldsymbol{f}+\boldsymbol{v}_1^{\mathrm{T}}\dot{\boldsymbol{v}}_1
\end{aligned}\tag{44}$$

https://doi.org/10.1017/S0263574718000061 Published online by Cambridge University Press

Substituting (37) and (44) into $\dot{V}_1$

$$\begin{aligned}\dot{V}_1 &= \dot{V}_0 + \tilde{\boldsymbol{d}}^{\mathrm{T}}\boldsymbol{\Gamma}_d\dot{\tilde{\boldsymbol{d}}} \\ &= \dot{V}_0 - \tilde{\boldsymbol{d}}^{\mathrm{T}}\boldsymbol{\Gamma}_d\boldsymbol{\Gamma}^{-1_d}(\boldsymbol{f}\,\|\boldsymbol{s}\| - \boldsymbol{a}\hat{\boldsymbol{d}}) \\ &= \dot{V}_0 - \tilde{\boldsymbol{d}}^{\mathrm{T}}\boldsymbol{f}\,\|\boldsymbol{s}\| + \tilde{\boldsymbol{d}}^{\mathrm{T}}\boldsymbol{a}\hat{\boldsymbol{d}}\end{aligned} \tag{45}$$

It is not difficult to see from (44) and (45) that $\dot{V}_1$ can be yielded as follow

$$\dot{V}_1 \le -\tilde{\boldsymbol{P}}^{\mathrm{T}}\boldsymbol{\Gamma}\tilde{\boldsymbol{P}} - \boldsymbol{s}^{\mathrm{T}}\boldsymbol{K}_s\boldsymbol{s} + \tilde{\boldsymbol{d}}^{\mathrm{T}}\boldsymbol{a}\hat{\boldsymbol{d}} + \boldsymbol{v}_1^{\mathrm{T}}\dot{\boldsymbol{v}}_1 \tag{46}$$

In a similar way, when $\|\boldsymbol{s}\| \le l_1$, the expression of $\dot{V}_1$ can also obtain the same inequality based on (34), (35) and (37)

Since

$$\frac{1}{2}(\boldsymbol{d} - \tilde{\boldsymbol{d}})^{\mathrm{T}}\boldsymbol{a}(\boldsymbol{d} - \tilde{\boldsymbol{d}}) \ge 0 \tag{47}$$

then it is easy to get

$$\tilde{\boldsymbol{d}}^{\mathrm{T}}\boldsymbol{a}\boldsymbol{d} \le \frac{1}{2}\boldsymbol{d}^{\mathrm{T}}\boldsymbol{a}\boldsymbol{d} + \frac{1}{2}\tilde{\boldsymbol{d}}^{\mathrm{T}}\boldsymbol{a}\tilde{\boldsymbol{d}} \tag{48}$$

Considering $\tilde{\boldsymbol{d}} = \boldsymbol{d} - \hat{\boldsymbol{d}}$, from (48), we have

$$\tilde{\boldsymbol{d}}^{\mathrm{T}}\boldsymbol{a}\hat{\boldsymbol{d}} \le \frac{1}{2}\boldsymbol{d}^{\mathrm{T}}\boldsymbol{a}\boldsymbol{d} - \frac{1}{2}\tilde{\boldsymbol{d}}^{\mathrm{T}}\boldsymbol{a}\tilde{\boldsymbol{d}} \tag{49}$$

From (38), (46) and (49), the following inequality is obtained.

$$\begin{aligned}\dot{V}_1 &\le -\tilde{\boldsymbol{P}}^{\mathrm{T}}\boldsymbol{\Gamma}\tilde{\boldsymbol{P}} - \boldsymbol{s}^{\mathrm{T}}\boldsymbol{K}_s\boldsymbol{s} + \frac{1}{2}\boldsymbol{d}^{\mathrm{T}}\boldsymbol{a}\boldsymbol{d} - \frac{1}{2}\tilde{\boldsymbol{d}}^{\mathrm{T}}\boldsymbol{a}\tilde{\boldsymbol{d}} - \boldsymbol{v}_1^{\mathrm{T}}(\boldsymbol{A}_1 + \boldsymbol{B}_1\boldsymbol{\Lambda}^{-1})\boldsymbol{v}_1 + \boldsymbol{v}_1^{\mathrm{T}}\boldsymbol{B}_1\boldsymbol{\Lambda}^{-1}\boldsymbol{v}_1 \\ &= -\boldsymbol{X}^{\mathrm{T}}\boldsymbol{\Theta}\boldsymbol{X} + \varepsilon \\ &\le -\lambda_{\min}(\boldsymbol{\Theta})\|\boldsymbol{X}\|^2 + \varepsilon\end{aligned} \tag{50}$$

where $\boldsymbol{X} = \begin{pmatrix}\boldsymbol{s}\\ \boldsymbol{v}_1\\ \tilde{\boldsymbol{P}}\\ \tilde{\boldsymbol{d}}\end{pmatrix}$, $\boldsymbol{\Theta} = \begin{pmatrix}\boldsymbol{K}_s & \frac{-\boldsymbol{B}_1\boldsymbol{\Lambda}^{-1}}{2} & \boldsymbol{0} & \boldsymbol{0}\\ \frac{-\boldsymbol{B}_1\boldsymbol{\Lambda}^{-1}}{2} & \boldsymbol{A}_1 + \boldsymbol{B}_1\boldsymbol{\Lambda}^{-1} & \boldsymbol{0} & \boldsymbol{0}\\ \boldsymbol{0} & \boldsymbol{0} & \boldsymbol{\Gamma} & \boldsymbol{0}\\ \boldsymbol{0} & \boldsymbol{0} & \boldsymbol{0} & \frac{1}{2}\boldsymbol{a}\end{pmatrix}$, $\varepsilon = \frac{1}{2}\lambda_{\min}(\boldsymbol{a})\|\boldsymbol{d}\|^2$ and $\lambda_{\min}(\cdot)$ represents the minimum eigenvalue values of the matrix.

Now, the sufficient conditions for $\boldsymbol{\Theta}$ to be positive definite in (50) is that the following inequality is satisfied

$$4\boldsymbol{K}_s(\boldsymbol{A}_1 + \boldsymbol{B}_1\boldsymbol{\Lambda}^{-1}) > (\boldsymbol{B}_1\boldsymbol{\Lambda}^{-1})^2 \tag{51}$$

Recalling the matrix form of (42), we can get

$$\frac{1}{2}\lambda_{\min}(\boldsymbol{\Omega})\|\boldsymbol{X}\|^2 \le \frac{1}{2}\boldsymbol{X}^{\mathrm{T}}\boldsymbol{\Omega}\boldsymbol{X} \le \frac{1}{2}\lambda_{\max}(\boldsymbol{\Omega})\|\boldsymbol{X}\|^2 \tag{52}$$

where $\lambda_{\max}(\cdot)$ is the maximum eigenvalue values of the matrix

From (50) and (52), we obtain

$$\begin{aligned}\dot{V}_1 &\le -\frac{2\lambda_{\min}(\boldsymbol{\Theta})}{\lambda_{\max}(\boldsymbol{\Omega})}V_1 + \varepsilon \\ &\le -\rho V_1 + \varepsilon\end{aligned} \tag{53}$$

where $\rho = \frac{2\lambda_{\min}(\boldsymbol{\Theta})}{\lambda_{\max}(\boldsymbol{\Omega})}$.

https://doi.org/10.1017/S0263574718000061 Published online by Cambridge University Press

According to the Lyapunov stability theory,[20] the slow subsystem is achieved to be stable. Moreover, for arbitrary $\boldsymbol{X}(0)$, as long as $t > t_0$, there exits

$$\|\boldsymbol{X}\| \leq \left\{ \frac{\lambda_{\max}(\boldsymbol{\Omega})}{\lambda_{\min}(\boldsymbol{\Omega})} \|\boldsymbol{X}(0)\|^2 e^{-\rho t} + \frac{2}{\lambda_{\min}(\boldsymbol{\Omega})\rho} \left(1 - e^{-\rho t}\right) \right\}^{1/2} \tag{54}$$

Therefore, all signals of tracking error are global uniformly ultimately bounded by using the proposed robust adaptive controller.

5.2. Stability analysis of the fast system

For the fast subsystem, consider the following Laypunov function candidate

$$V_2 = \mu \left(\frac{1}{2} \dot{\boldsymbol{\eta}}^{\mathrm{T}} \dot{\boldsymbol{\eta}} + \frac{1}{2} \boldsymbol{\eta}^{\mathrm{T}} \boldsymbol{k}_{\mathrm{p}} \boldsymbol{\eta} + \frac{1}{2} \boldsymbol{v}_2^{\mathrm{T}} \boldsymbol{k}_{\mathrm{v}} \boldsymbol{B}_2^{-1} \boldsymbol{v}_2 + \chi \boldsymbol{\eta}^{\mathrm{T}} \dot{\boldsymbol{\eta}} - \chi \boldsymbol{v}_2^{\mathrm{T}} \dot{\boldsymbol{\eta}} \right) \tag{55}$$

where χ is a sufficiently small positive constant, which is not used in the controller but only for stability proof purposes.

Notice that (55) can be rewritten in the form of matrix as $V_2 = \mu \boldsymbol{Y}^{\mathrm{T}} \boldsymbol{P}_1 \boldsymbol{Y}$, where $\boldsymbol{Y} = \begin{pmatrix} \boldsymbol{\eta} \\ \dot{\boldsymbol{\eta}} \\ \boldsymbol{v}_2 \end{pmatrix}$, $\boldsymbol{P}_1 = \begin{pmatrix} \frac{\boldsymbol{K}_{\mathrm{p}}}{2} & \mathbf{I}\frac{\chi}{2} & \mathbf{0} \\ \mathbf{I}\frac{\chi}{2} & \mathbf{I}\frac{1}{2} & -\mathbf{I}\frac{\chi}{2} \\ 0 & -\mathbf{I}\frac{\chi}{2} & \frac{\boldsymbol{k}_{\mathrm{v}} \boldsymbol{B}_2^{-1}}{2} \end{pmatrix}$. It can be found that V_2 will be positive definite if $\boldsymbol{P}_1$ is a positive definite matrix, i.e., the following two inequalities (56) and (57) are satisfied:

$$\sqrt{\lambda_{\min}(\boldsymbol{k}_{\mathrm{p}})} > \chi \tag{56}$$

$$\sqrt{\frac{\lambda_{\min}(\boldsymbol{k}_{\mathrm{p}} \boldsymbol{k}_{\mathrm{v}} \boldsymbol{B}_2^{-1})}{\lambda_{\max}(\boldsymbol{k}_{\mathrm{p}} + \boldsymbol{k}_{\mathrm{p}})}} > \chi \tag{57}$$

Substituting the fast control law in (40), the relationship between $\boldsymbol{u}_{\mathrm{f}}$ and $\boldsymbol{u}_{\mathrm{f}}^*$ in (18), and the velocity error estimation signals in (41) into the reshaped fast system (17), the elastic torque error can be obtained as

$$\ddot{\boldsymbol{\eta}} + \boldsymbol{k}_{\mathrm{p}} \boldsymbol{\eta} + \boldsymbol{k}_{\mathrm{v}} \boldsymbol{v}_2 = \mathbf{0} \tag{58}$$

Differentiating V_2 with respect to the fast scale time $\delta = \frac{t}{\mu}$ and substituting (58)

$$\begin{aligned} \dot{V}_2 &= \dot{\boldsymbol{\eta}}^{\mathrm{T}} \ddot{\boldsymbol{\eta}} + \boldsymbol{\eta}^{\mathrm{T}} \boldsymbol{k}_{\mathrm{p}} \dot{\boldsymbol{\eta}} + \boldsymbol{v}_2^{\mathrm{T}} \boldsymbol{k}_{\mathrm{v}} \boldsymbol{B}_2^{-1} \dot{\boldsymbol{v}}_2 + \chi \boldsymbol{\eta}^{\mathrm{T}} \ddot{\boldsymbol{\eta}} + \chi \dot{\boldsymbol{\eta}}^{\mathrm{T}} \dot{\boldsymbol{\eta}} - \chi \dot{\boldsymbol{v}}_2^{\mathrm{T}} \dot{\boldsymbol{\eta}} - \chi \boldsymbol{v}_2^{\mathrm{T}} \ddot{\boldsymbol{\eta}} \\ &= -\boldsymbol{v}_2^{\mathrm{T}} \boldsymbol{k}_{\mathrm{v}} \boldsymbol{B}_2^{-1} \boldsymbol{v}_2 - \chi \boldsymbol{\eta}^{\mathrm{T}} \boldsymbol{k}_{\mathrm{p}} \boldsymbol{\eta} - \chi \boldsymbol{\eta}^{\mathrm{T}} \boldsymbol{k}_{\mathrm{v}} \boldsymbol{v}_2 + \chi \dot{\boldsymbol{\eta}}^{\mathrm{T}} \dot{\boldsymbol{\eta}} + \chi \boldsymbol{v}_2^{\mathrm{T}} \boldsymbol{A}_2^{\mathrm{T}} \dot{\boldsymbol{\eta}} - \chi \dot{\boldsymbol{\eta}}^{\mathrm{T}} \boldsymbol{B}_2^{\mathrm{T}} \dot{\boldsymbol{\eta}} + \chi \boldsymbol{v}_2^{\mathrm{T}} \boldsymbol{k}_{\mathrm{p}} \boldsymbol{\eta} + \chi \boldsymbol{v}_2^{\mathrm{T}} \boldsymbol{k}_{\mathrm{v}} \boldsymbol{v}_2 \end{aligned} \tag{59}$$

https://doi.org/10.1017/S0263574718000061 Published online by Cambridge University Press

According to Rayleigh–Ritz inequality,[17] the following inequalities can be established:

$$
\begin{aligned}
-\boldsymbol{v}_2^{\mathrm{T}}\boldsymbol{k}_{\mathrm{v}}\boldsymbol{B}_2^{-1}\boldsymbol{A}_1\boldsymbol{v}_2 &\le -\lambda_{\min}(\boldsymbol{k}_{\mathrm{v}}\boldsymbol{B}_2^{-1}\boldsymbol{A}_1)\|\boldsymbol{v}_2\|^2\\
-\chi\boldsymbol{\eta}^{\mathrm{T}}\boldsymbol{k}_{\mathrm{p}}\boldsymbol{\eta} &\le -\chi\lambda_{\min}(\boldsymbol{k}_{\mathrm{p}})\|\boldsymbol{\eta}\|^2\\
-\chi\boldsymbol{\eta}^{\mathrm{T}}\boldsymbol{k}_{\mathrm{v}}\boldsymbol{v}_2 &\le -\chi\sigma_{\min}(\boldsymbol{k}_{\mathrm{v}})\,\|\boldsymbol{\eta}\|\,\|\boldsymbol{v}_2\|\\
\chi\dot{\boldsymbol{\eta}}^{\mathrm{T}}\dot{\boldsymbol{\eta}} &\le \chi\|\dot{\boldsymbol{\eta}}\|^2\\
\chi\boldsymbol{v}_2^{\mathrm{T}}\boldsymbol{A}_2^{\mathrm{T}}\dot{\boldsymbol{\eta}} &\le \chi\sigma_{\max}(\boldsymbol{A}_2^{\mathrm{T}})\,\|\boldsymbol{v}_2\|\,\|\dot{\boldsymbol{\eta}}\|\\
-\chi\dot{\boldsymbol{\eta}}^{\mathrm{T}}\boldsymbol{B}_2^{\mathrm{T}}\dot{\boldsymbol{\eta}} &\le -\chi\lambda_{\min}(\boldsymbol{B}_2^{\mathrm{T}})\|\dot{\boldsymbol{\eta}}\|^2\\
\chi\boldsymbol{v}_2^{\mathrm{T}}\boldsymbol{k}_{\mathrm{p}}\boldsymbol{\eta} &\le \chi\sigma_{\max}(\boldsymbol{k}_{\mathrm{p}})\,\|\boldsymbol{v}_2\|\,\|\boldsymbol{\eta}\|\\
\chi\boldsymbol{v}_2^{\mathrm{T}}\boldsymbol{k}_{\mathrm{v}}\boldsymbol{v}_2 &\le \chi\lambda_{\max}(\boldsymbol{k}_{\mathrm{v}})\|\boldsymbol{v}_2\|^2
\end{aligned}
$$

where $\sigma_{\max}(\cdot)$, $\sigma_{\min}(\cdot)$ denote the largest and smallest singular value of the corresponding matrices, respectively.

By using the inequalities above in sequence, $\dot{V}_2$ in (59) can be written as

$$\dot{V}_2 \le -\boldsymbol{C}^{\mathrm{T}}\boldsymbol{P}_2\boldsymbol{C} \tag{60}$$

where

$$\boldsymbol{C} = \begin{pmatrix}\|\boldsymbol{\eta}\|\\ \|\dot{\boldsymbol{\eta}}\|\\ \|\boldsymbol{v}\|\end{pmatrix},\ \boldsymbol{P}_2 = \begin{pmatrix}\chi\lambda_{\min}(\boldsymbol{k}_{\mathrm{p}}) & 0 & \frac{\chi(\sigma_{\min}(\boldsymbol{k}_{\mathrm{v}})-\sigma_{\max}(\boldsymbol{k}_{\mathrm{p}}))}{2}\\ 0 & \chi\lambda_{\min}(\boldsymbol{B}_2)-\chi & \frac{\chi\sigma_{\max}(\boldsymbol{A}_2)}{2}\\ \frac{\chi(\sigma_{\min}(\boldsymbol{k}_{\mathrm{v}})-\sigma_{\max}(\boldsymbol{k}_{\mathrm{p}}))}{2} & \frac{\chi\sigma_{\max}(\boldsymbol{A}_2)}{2} & \lambda_{\min}(\boldsymbol{k}_{\mathrm{v}}\boldsymbol{B}_2^{-1}\boldsymbol{A}_2)-\chi\lambda_{\max}(\boldsymbol{k}_{\mathrm{v}})\end{pmatrix}.$$

To ensure $\dot{V}_2$ is negative definite, $\boldsymbol{P}_2$ should be positive definite, i.e.

$$\lambda_{\min}(\boldsymbol{B}_2) > 1 \tag{61}$$

$$\frac{4\lambda_{\min}(\boldsymbol{k}_{\mathrm{p}})(\lambda_{\min}(\boldsymbol{B}_2)-1)\lambda_{\min}(\boldsymbol{k}_{\mathrm{v}}\boldsymbol{B}_2^{-1}\boldsymbol{A}_2)}{\sigma_{\max}^2(\boldsymbol{A}_2)\lambda_{\min}(\boldsymbol{k}_{\mathrm{p}})+(\sigma_{\min}(\boldsymbol{k}_{\mathrm{v}})-\sigma_{\max}(\boldsymbol{k}_{\mathrm{p}}))^2(\lambda_{\min}(\boldsymbol{B}_2)-1+4\lambda_{\min}(\boldsymbol{K}_{\mathrm{p}})\lambda_{\max}(\boldsymbol{k}_{\mathrm{v}})(\lambda_{\min}(\boldsymbol{B}_2)-1)} > \chi \tag{62}$$

Therefore, if the above conditions (56), (57), (61) and (62) hold, the asymptotic stability of the fast subsystem is guaranteed.

5.3. Stability analysis of the composite system

The stability of the slow subsystem and the fast subsystem has been discussed in the previous subsections. However, the stability of the individual subsystems does not guarantee the stability of the total control system. This subsection will focus on the stability analysis of the whole composite system in detail.

Consider the following composite Lyapunov function candidate[17]

$$V = b_1V_1 + b_2V_2 \tag{63}$$

where V_1 denotes the Lyapunov function candidate for the slow subsystem given in (28) and V_2 denotes that for the fast subsystem given in (17), and both b_1 and b_2 are positive constants. As presented in ref. [17], it can be selected that $b_1 = b_2 = 1$. Obviously, $V = b_1V_1 + b_2V_2$ is positive definite based on the previous proof.

Then, take the derivative of V with respect to time, it is obtained that

$$\dot{V} = b_1\dot{V}_1 + b_2\dot{V}_2 \tag{64}$$

https://doi.org/10.1017/S0263574718000061 Published online by Cambridge University Press

Importantly, the similar method in Section 5.1 can be used here to prove the stability of the first part $\dot{V}_1$ in (63). Note that there is an important difference that (26) should be replaced by (24) and then be substituted into $\dot{V}_1$, due to that the total system is represented by (24) and (25). The stability analysis of the fast subsystem is exactly same as the stability analysis in the Section 5.2. Consequently, it is easy to obtain that $\dot{V}$ is negative definite, so as to conclude that the whole composite system is asymptotically stable.

6. Simulations

In this section, to verify the proposed robust adaptive OFT controller (named as RA-OFTC), simulation comparisons with the robust adaptive controller (named as RAC) are presented on a two-link flexible-joint robot manipulators in ref. [23] see Fig. 2.

The functions of $\boldsymbol{M}(\boldsymbol{q}), \boldsymbol{C}(\boldsymbol{q}, \dot{\boldsymbol{q}}), \boldsymbol{G}(\boldsymbol{q})$ are expressed in terms of the elements of the parameter vector $\boldsymbol{P} = (\, p_1 \quad p_2 \quad p_3 \quad p_4 \quad p_5\,)^{\mathrm{T}}$ as follows:

$$\boldsymbol{M}(\boldsymbol{q}) = \begin{bmatrix} p_1 + p_2 + 2p_3 \cos q_2 & p_2 + p_3 \cos q_2 \\ p_2 + p_3 \cos q_2 & p_2 \end{bmatrix},$$

$$\boldsymbol{C}(\boldsymbol{q}, \dot{\boldsymbol{q}}) = \begin{bmatrix} -p_3 \dot{q}_2 \sin q_2 & -p_3(\dot{q}_1 + \dot{q}_2) \sin q_2 \\ p_3 \dot{q}_1 \sin q_2 & 0 \end{bmatrix},$$

$$\boldsymbol{G}(\boldsymbol{q}) = \begin{bmatrix} [p_4 \cos q_1 + p_5(p_1 + p_2)]g \\ p_5 \cos(p_1 + p_2) g \end{bmatrix},$$

$$\boldsymbol{J} = \mathrm{diag}\{0.1, 0.1\}, \ \ g = 9.81.$$

Without loss of generality, the general expressions for the desired position trajectories are given as

$$q_{\mathrm{d}1} = 1/(10\pi)\sin(10\pi t + \pi/6)\ \mathrm{rad},$$
$$q_{\mathrm{d}2} = 1/(10\pi)\sin(10\pi t + \pi/6)\ \mathrm{rad}.$$

The saturation function $\mathrm{sat}(\boldsymbol{s})$ is chosen as

$$\mathrm{sat}(\boldsymbol{s}) = \begin{cases} \dfrac{\pi}{2}\mathrm{sign}(\boldsymbol{s}), & \|\boldsymbol{s}\| > 2 \\ \dfrac{\pi}{4}\boldsymbol{s}, & \|\boldsymbol{s}\| \le 2 \end{cases} \tag{65}$$

The control law of RAC is given by (66)–(68):

$$\boldsymbol{u}''_{\mathrm{s}} = \hat{\boldsymbol{M}}\ddot{\boldsymbol{q}}_{\mathrm{r}} + \hat{\boldsymbol{C}}\dot{\boldsymbol{q}}_{\mathrm{r}} + \hat{\boldsymbol{G}} + \boldsymbol{K}_s \boldsymbol{s} + \boldsymbol{\Phi} \tag{66}$$

$$\boldsymbol{\Phi} = \hat{\boldsymbol{d}}^{\mathrm{T}} \boldsymbol{f} \cdot \mathrm{sign}(\boldsymbol{s}) \tag{67}$$

$$\dot{\hat{\boldsymbol{P}}} = \boldsymbol{\Gamma}^{-1}\boldsymbol{Y}\boldsymbol{s}, \ \dot{\hat{\boldsymbol{d}}} = \boldsymbol{\Gamma}_{\boldsymbol{d}}{}^{-1}(\boldsymbol{f}\|\boldsymbol{s}\|^2 - \boldsymbol{a}\hat{\boldsymbol{d}}) \tag{68}$$

$$\boldsymbol{u}''_{\mathrm{f}} = \boldsymbol{K}_{\mathrm{P}}\boldsymbol{\eta} + \boldsymbol{K}_{\mathrm{D}}\dot{\boldsymbol{\eta}} \tag{69}$$

where $\boldsymbol{u}''_{\mathrm{s}}$ and $\boldsymbol{u}''_{\mathrm{f}}$ are the slow and fast control law of RAC, respectively.

To make fair comparisons, same value for the same parameters in two controllers is selected:

$$\boldsymbol{\Gamma} = \mathrm{diag}\{1000, 1000, 1000, 1000, 1000\}, \ \boldsymbol{K}_s = \mathrm{diag}\{80, 80\}, \ \boldsymbol{\Lambda} = \mathrm{diag}\{20, 20\}$$

$$\boldsymbol{\Gamma}_{\boldsymbol{d}} = \mathrm{diag}\{20, 20, 20\}, \ \boldsymbol{K}_{\mathrm{P}} = \mathrm{diag}\{1, 1\}, \ \boldsymbol{K}_{\mathrm{D}} = \mathrm{diag}\{0.01, 0.01\}$$

$$\lambda_{\mathrm{c}} = 1, \ m_1 = \frac{\pi}{2}, \ \boldsymbol{A}_1 = \boldsymbol{A}_2 = \boldsymbol{B}_1 = \boldsymbol{B}_2 = \mathrm{diag}\{1000, 1000\}.$$

Furthermore, to test the anti-disturbance capability of the controllers, man-made square-wave pulse torques are applied as external disturbances during the time of 1 second to 2 second, with the

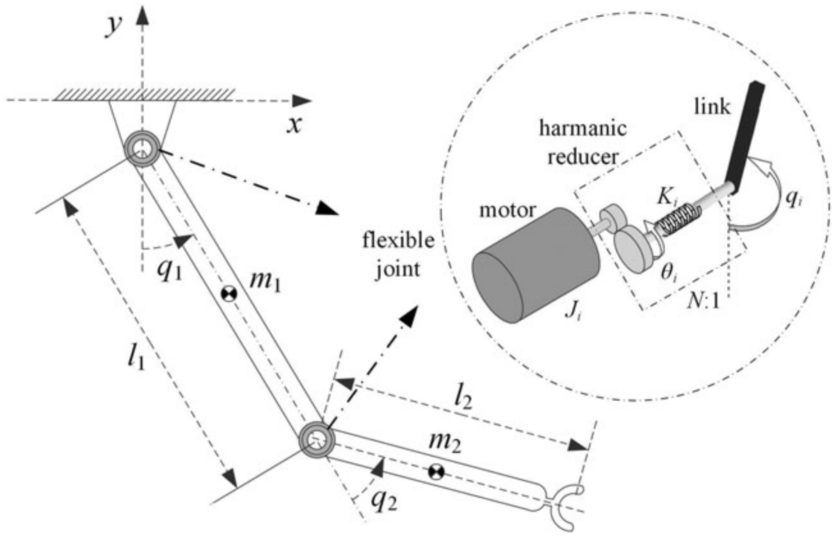

Fig. 2. A two-link flexible-joint robot manipulator.

amplitudes of 3 Nm to the first joint and 2 Nm to the second one. To make comprehensive performance assessment of the controllers, the following criteria[24,25] are adopted:

Adjusting time—a period from the start to the moment tracking error $\boldsymbol{e}$ falls into the area of ±5% of the final value.

Overshoot—the maximum value of $|e_i|$ during the adjusting procedure.

Recovery time—a period since the end of disturbances to the moment tracking error $|e_i|$ falls into the area of±5%of the final value.

Maximum deviation—the maximum value of $|e_i|$ from the start of disturbances to the end of the recovery procedure.

Maximum torque—the maximum value of torque input $|\tau_i|$ during the whole procedure.

RMS—root mean square, it indicates the average performance in respect of tracking errors, which is defined as

$$\mathrm{RMS}(e_i) = \sqrt{\int_0^T |e_i|^2 dt/T}, \ i = 1, 2. \tag{70}$$

$$\mathrm{RMS}(\boldsymbol{e}) = \sqrt{\int_0^T \|\boldsymbol{e}\|^2 dt/T}. \tag{71}$$

From the position tracking error curves in Figs. 3 and 4, it can be found that the proposed controller (RA-OFTC) has smaller oscillation amplitude compared to the controller (RAC) in ref. [23], due to that an improved linear parameterization expression by (31) is adopted in the control law, which makes the adaptive parameters estimation more accurate. As shown in Table I, the RMS($\boldsymbol{e}$) in ours (RA-OFTC) decreases by 9.87% at the first joint, 9.38% at the second joint and 9.55% on the whole in comparison with those of the controller (RAC) in ref. [23], respectively.

When there comes out a sudden external torque disturbance at the joints, the tracking errors expand a bit and soon fall into the normal range in our controller (RA-OFTC). As shown in Table I, RA-OFTC has a shorter adjusting time and recovery time, the smaller overshoot, the smaller maximum deviation compared with RAC, representing superior capacity of dynamic response and anti-disturbance.

Specially, as shown in Figs. 5 and 6, our controller (RA-OFTC) has the much smaller initial torque, and is only 26.82% at the first joint and 41.66% at the second joint of those of the controller in ref. [23].

https://doi.org/10.1017/S0263574718000061 Published online by Cambridge University Press

Table I. Comparisons of controller.

Parameter		RA-OFTC	RAC
Adjusting time (s)	Link 1	0.39	0.42
	Link 2	0.35	0.38
Overshoot (10^{-3}rad)	Link 1	0.85	1.49
	Link 2	0.26	1.03
Recovery time (s)	Link 1	0.53	0.74
	Link 2	0.50	0.69
Maximum deviation (10^{-3}rad)	Link 1	2.50	2.93
	Link 2	1.44	1.97
Maximum torque (Nm)	Joint 1	93.55	348.82
	Joint 2	60.42	145.04
RMS (rad)	e_1	0.0475	0.0527
	e_2	0.0406	0.0448
	$\boldsymbol{e}$	0.0625	0.0691

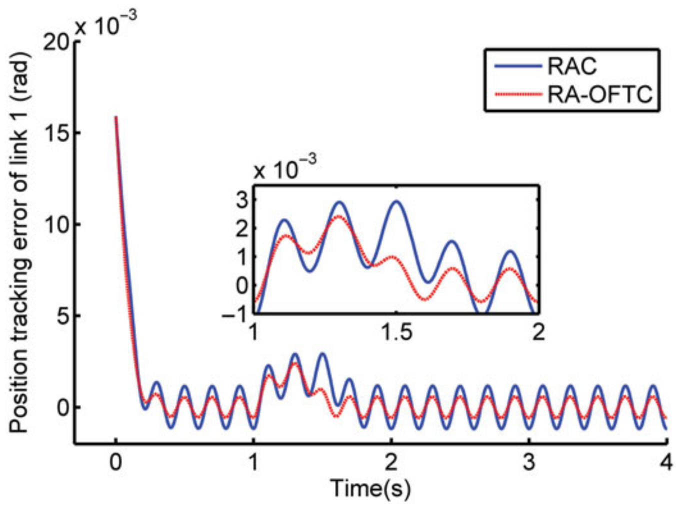

Fig. 3. Tracking error of link 1.

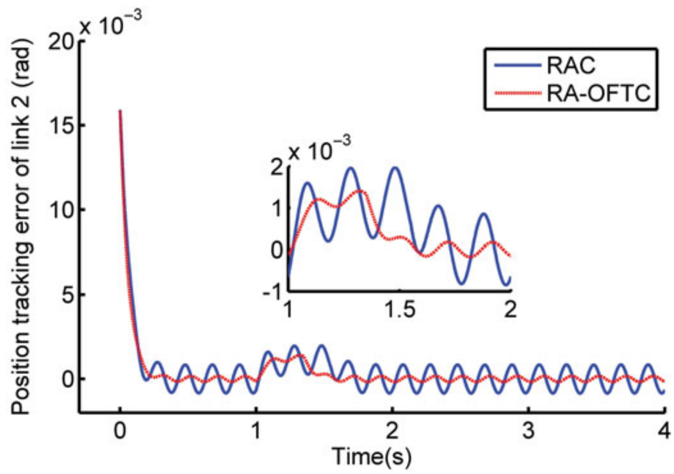

Fig. 4. Tracking error of link 2.

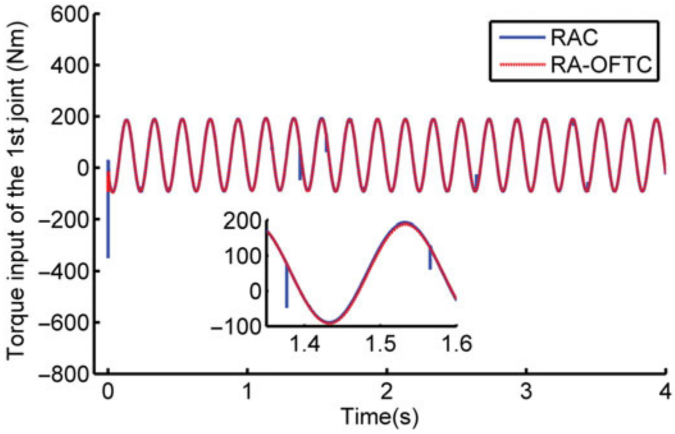

Fig. 5. Torque input of joint 1.

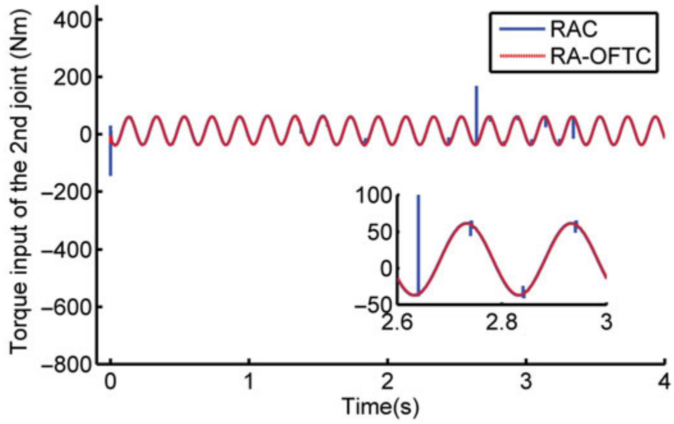

Fig. 6. Torque input of joint 2.

Moreover, there appears some sharp torque pulses in the controller (RAC) in ref. [23], due to that the saturation function $\mathrm{sat}(\boldsymbol{s})$ is adopted in its control law, while a continuous saturation function that can avoid the sharp-pulse phenomenon of the torque output is applied in ours (RA-OFTC).

More importantly, approximate differential filtering technique is applied to achieve OFT control in RA-OFTC, which avoids the velocity measurements for both links and joint motors. What's more, the approximate differential filter is applied in the controllers, which can alleviate the initial input torque too large in some extend by choosing the appropriate filter parameters.

7. Conclusions

This work clearly states a detailed design of a robust adaptive OFT control method for flexible-joint robot manipulators with parameter uncertainties and external disturbances. It is highlighted by an improved linear parameterization expression and a class of continuous saturation function invoked in the robust adaptive control law, as well as an approximate differential filter adopted to eliminate the velocity measurements for both links and joint motors in slow and fast subsystems that decoupled by singular perturbation theory. In addition, comprehensive stability analysis of both subsystems and whole composite system is also made.

The simulation results demonstrate that, considering the problems of parameter uncertainties and external disturbances, by the proposed controller, resistance ability to external disturbance is enhanced, tracking errors of links are decreased and the sharp-pulse phenomenon of the torque output is avoided effectively, which guarantees a superior dynamic performance and makes the proposed scheme as a valuable reference for other similar robotic systems.

https://doi.org/10.1017/S0263574718000061 Published online by Cambridge University Press

Acknowledgements

This work was sponsored in part by the National Natural Science Foundation of China under Grant no. 61203337, the State Scholarship Fund under Grant no. 201406635025, the Specialized Research Fund for the Doctoral Program of Higher Education under Grant no. 20120075120009, the Natural Science Foundation of Shanghai under Grant no. 17ZR1400100, the DHU Distinguished Young Professor Program under Grant no. B201309, the Fundamental Research Funds for the Central Universities under Grant no. 2232012D3-18, and the Chen Guang project supported by Shanghai Municipal Education Commission and Shanghai Education Development Foundation under Grant no. 13CG29.

References

1. C. T. Kiang, A. Spowage and C. K. Yoong, “Review of control and sensor system of flexible manipulator,” *J. Intell. Robot. Syst.* **77**(1), 187–213 (2015).
2. A. Izadbakhsh, “Robust control design for rigid-link flexible-joint electrically driven robot subjected to constraint: Theory and experimental verification,” *Nonlinear Dyn.* **85**(2), 1–15 (2016).
3. J. Lessard, P. Bigras, Z. Liu *et al*., “Characterization, Modeling and vibration control of a flexible joint for a robotic system,” *J. Vib. Control* **20**(6), 943–960 (2012).
4. K. Nanos and E. G. Papadopoulos, “On the dynamics and control of flexible joint space manipulators,” *Control Eng. Pract.* **45**, 230–243 (2015).
5. J. J. E. Slotine and W. Li, “On the adaptive control of robot manipulators,” *Int. J. Robot. Res.* **6**(3), 49–59 (1987).
6. M. W. Spong, “Modeling and control of elastic joint robots,” *J. Dyn. Syst. Meas. Control* **109**(4), 310–318 (1987).
7. M. Spong, K. Khorasani and P. V. Kokotovic, “An integral manifold approach to the feedback control of flexible joint robots,” *IEEE J. Robot. Autom.* **3**(4), 291–300 (1987).
8. S. S. Ge, “Adaptive controller design for flexible joint manipulators,” *Automatica* **32**(2), 273–278 (1996).
9. S. Ulrich, J. Z. Sasiadek and I. Barkana, “Modeling and direct adaptive control of a flexible-joint manipulator,” *J. Guid. Control Dyn.* **35**(1), 25–39 (2012).
10. Z. G. Liu and J. M. Huang, “A new adaptive tracking control approach for uncertain flexible joint robot system,” *Int. J. Autom. Comput.* **12**(5), 559–566 (2015).
11. X. Yang, S. S. Ge and W. He, “Dynamic modelling and adaptive robust tracking control of a space robot with two-link flexible manipulators under unknown disturbances,” *Int. J. Control* in press (DOI: 10.1080/00207179.2017.1300837), (2017).
12. M. M. Fateh and S. Khorashadizadeh, “Robust control of electrically driven robots by adaptive fuzzy estimation of uncertainty,” *Nonlinear Dyn*. **69**(3), 1465–1477 (2012).
13. J. P. Kolhe, M. Shaheed, T. S. Chandar *et al*., “Robust control of robot manipulators based on uncertainty and disturbance estimation,” *Int. J. Robust Nonlinear* **23**(1), 104–122 (2013).
14. A. Loría and S. Avila-Becerril, “Output-Feedback Global Tracking Control of Robot Manipulators with Flexible Joints,” *IEEE, American Control Conference* (2014) pp. 4032–4037.
15. S. J. Yoo, J. B. Park and Y. H. Choi, “Adaptive output feedback control of flexible-joint robots using neural networks: dynamic surface design approach,” *IEEE Trans. Neural Netw.* **19**(10), 1712–1726 (2008).
16. S. J. Yoo, J. B. Park and Y. H. Choi, “Output feedback dynamic surface control of flexible-joint robots,” *Int. J. Control Autom.* **6**(2), 223 (2008).
17. M. A. Khosravi and H. D. Taghirad, “Dynamic modeling and control of parallel robots with elastic cables: singular perturbation approach,” *IEEE Trans. Robot.* **30**(3), 694–704 (2014).
18. D. W. Wang, “Trajectory Tracking for Manipulators with Flexible Joints Using Link Variable Feedback,” *Proceedings of the 32nd IEEE Conference on IEEE Decision and Control* (1993) pp. 633–637.
19. R. Kelly, R. Ortega, A. Ailon *et al*., “Global regulation of flexible joint robots using approximate differentiation,” *IEEE Trans. Autom. Control* **39**(6), 1222–1224 (1994).
20. J. K. Liu, *Robot Control System Design and Matlab Simulation* (Tsinghua University Press, Beijing, 2008).
21. F. Raouf, S. Mohamad, S. Maarouf *et al*., “Distributed adaptive control strategy for flexible link manipulators,” *Robotica* **35**(7), 1562–1584 (2017).
22. S. Gayaka, L. Lu and B. Yao, “Global stabilization of a chain of integrators with input saturation and disturbances: A new approach,” *Automatica* **48**(7), 1389–1396 (2012).
23. J. Peng, J. Yu and J. Wang, “Robust adaptive tracking control for nonholonomic mobile manipulator with uncertainties,” *ISA Trans*. **53**(4), 1035–1043 (2014).
24. H. Liu, K. Hao and X. Lai, “Fuzzy saturated output feedback tracking control for robot manipulators: A singular perturbation theory based approach,” *Int. J. Adv. Robot. Syst.* **8**(4), 43–53 (2011).
25. H. Liu and S. Zhu, “A generalized trajectory tracking controller for robot manipulators with bounded inputs,” *J. Zhejiang Univ. Sci. A* **10**(10), 1500–1508 (2009).

https://doi.org/10.1017/S0263574718000061 Published online by Cambridge University Press